

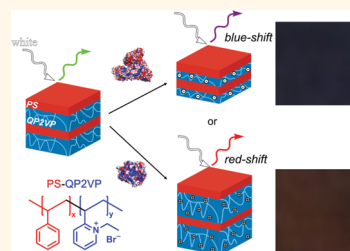
Responsive Block Copolymer Photonics Triggered by Protein–Polyelectrolyte Coacervation

Yin Fan,[†] Shengchang Tang,[†] Edwin L. Thomas,^{*,‡} and Bradley D. Olsen^{*,†}

[†]Department of Chemical Engineering, Massachusetts Institute of Technology, 77 Massachusetts Avenue, Cambridge, Massachusetts 02139, United States and

[‡]Department of Materials Science and Nanoengineering and Department of Chemical and Biomolecular Engineering, Rice University, 600 Main MS-364, Houston, Texas 77005, United States

ABSTRACT Ionic interactions between proteins and polyelectrolytes are demonstrated as a method to trigger responsive transitions in block copolymer (BCP) photonic gels containing one neutral hydrophobic block and one cationic hydrophilic block. Poly(2-vinylpyridine) (P2VP) blocks in lamellar poly(styrene-*b*-2-vinylpyridine) block copolymer thin films are quaternized with primary bromides to yield swollen gels that show strong reflectivity peaks in the visible range; exposure to aqueous solutions of various proteins alters the swelling ratios of the quaternized P2VP (QP2VP) gel layers in the PS-QP2VP materials due to the ionic interactions between proteins and the polyelectrolyte. Parameters such as charge density, hydrophobicity, and cross-link density of the QP2VP gel layers as well as the charge and size of the proteins play significant roles on the photonic responses of the BCP gels. Differences in the size and pH-dependent charge of proteins provide a basis for fingerprinting proteins based on their temporal and equilibrium photonic response. The results demonstrate that the BCP gels and their photonic effect provide a robust and visually interpretable method to differentiate different proteins.



KEYWORDS: block copolymer · photonic gel · proteins · polyelectrolytes · coacervation

Structural color is one of the primary mechanisms used in nature to produce the brilliant colors found across the animal kingdom.^{2,3} Bird feathers,^{4,5} butterfly wings,^{6,7} beetles,⁸ and squid⁹ all use structural color originating from photonic crystals to produce elegant iridescent hues and color-changing effects. The physics of such systems is well understood: periodic variations in the refractive index on a length scale on the order of the wavelength of light create constructive interference that leads to a partial photonic band gap in the material, creating sharp peaks in reflectivity that lead to a perceived color in the absence of optical absorption.¹⁰

Many previous studies^{11–16} have demonstrated the ability of block copolymers (BCPs) to exhibit structural color (reflectivity) when the repeat domain size in the materials approaches the wavelength of visible light. While such structural color can be achieved in the neat state using extremely high molar mass materials,^{17,18} swelling of lower molar mass polymers provides an alternate route to achieve domain spacings in the 100s of

nanometer range.^{11,12} In these materials, typically one block is insoluble and glassy to prevent dissolution of the copolymer, while a second block is highly swollen to yield a large domain spacing. The swelling of these block copolymer gels is responsive to a variety of stimuli, including temperature,^{19,20} salinity,¹⁵ and pH,²¹ enabling responsive changes in structural color triggered *via* the swelling/deswelling of the gel block.¹⁶

In addition to modulating the swelling of polymers due to changes in solvent quality, it is possible to cause deswelling or precipitation of a polymer due to the formation of strong associations with other macromolecules, such as by counterion coacervation. Macrophase separation of complexes formed between two oppositely charged polyelectrolytes in solution is driven largely by an increase in entropy that results from the displacement of small counterions by the formation of the macromolecular ionic complex.^{22–26} This process can be applied

* Address correspondence to bdolsen@mit.edu, elt@rice.edu.

Received for review August 14, 2014 and accepted October 22, 2014.

Published online November 13, 2014
10.1021/nn504565r

© 2014 American Chemical Society

to nanomaterial construction, including the formation of hydrogels,²⁷ self-assembly of micelles or nanoparticles,²⁸ and templated self-assembly.²⁹ Proteins form coacervates with polyelectrolytes in solutions,³⁰ where the density of the protein–polymer complex far exceeds the average polymer concentration in the system. The coacervation effect has been used for enzyme immobilization and protein delivery, separation, and purification.³⁰

Herein, it is shown that in lamellar BCPs composed of a polyelectrolyte block, the gel layers swell/deswell when the BCP gels are exposed to protein solutions that form coacervates with the polyelectrolyte block. The structural color of a BCP gel is related to the swelling ratio of the gel layers and can therefore be used to measure the effect of the ionic interactions between the protein and the polyelectrolyte block. The fast and sensitive responses of the BCP gels provide a quick and visually interpretable method to differentiate proteins by their interactions with polyelectrolytes. In addition to the steady-state photonic responses, the real-time spectra collected using a high-speed spectrometer can help determine the transport of the proteins in the lamellar BCP gels. The charge density, hydrophobicity, and cross-link density of the quaternized poly(2-vinylpyridine) (QP2VP) gel block all have a significant impact on the resulting

photonic effect, as do the shape and charge of the protein.

RESULTS AND DISCUSSION

The block copolymer photonic gels show a characteristic response based upon the pH-dependent charge of an analyte protein, providing a potential mechanism for fingerprinting unknown proteins. When block copolymer gels with a QP2VP block are brought into contact with protein solutions, the protein may yield a red or blue shift in the reflectivity of the structure due to changes in gel swelling (Figure 1). The sign of the protein's charge is the largest factor controlling the protein–polymer interaction; therefore, this interaction depends upon the relationship between the protein's isoelectric point (*p*_I) and the solution pH. When a protein is above its isoelectric point, it has a net negative charge, and it can form a coacervate with the polycationic domains of the block copolymer. For example, bovine serum albumin (BSA) has a *p*_I of 5.3, so across the buffered pH range of 7–9 in Tris buffer, it always has a negative charge. When photonic gels are swollen in buffer then immersed in a 1 wt % BSA solution, they demonstrate strong blue shifts in the peak reflectivity (Figure 2A,B). Simply mixing BSA and QP2VP in solution shows that they interact strongly to form a coacervate phase (Supporting Information Figure S1).

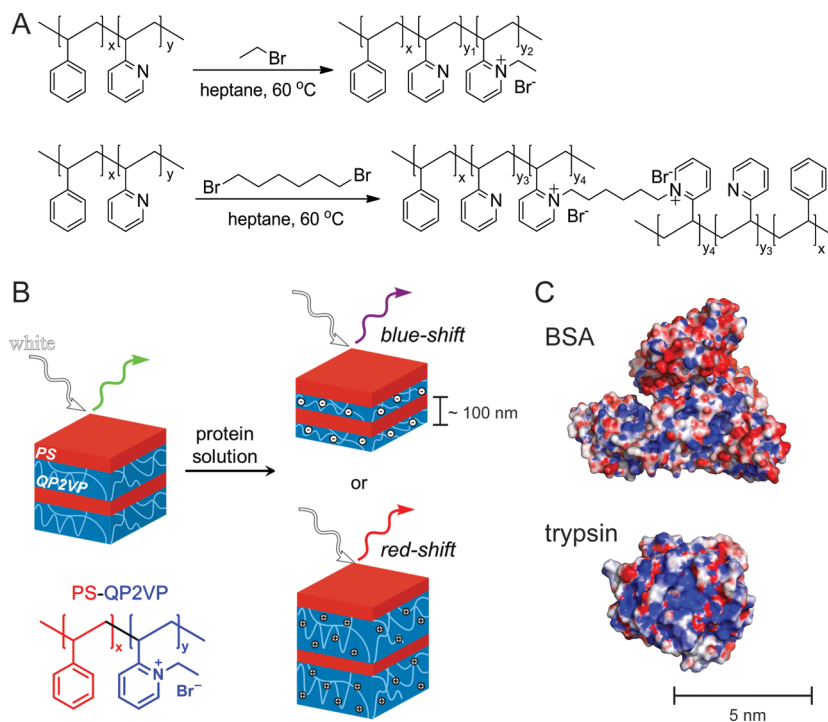


Figure 1. (A) Quaternization reactions on the pyridine groups in annealed lamellar poly(styrene-*b*-2-vinylpyridine) (PS-P2VP) films with bromoethane (EtBr) or dibromohexane (DBH). EtBr converts the P2VP into a polycation block that swells in water where the quaternized monomers are randomly distributed throughout the block. DBH randomly quaternizes and cross-links the P2VP into a network. (B) Schematic of the lamellar PS-QP2VP photonic gel and its two possible behaviors (swelling/contraction) in protein solutions. (C) Structure and electrostatic potential map ($\pm 10 k_B T/e_c$) of BSA (PDB file 4F5S) and trypsin (PDB file 1S81) at pH 7 and 10 mM ionic strength. Results are generated from solving the linearized Poisson–Boltzmann equation using the Adaptive Poisson–Boltzmann Solver.¹ Negative charges are shown in red, and positive charges are shown in blue.

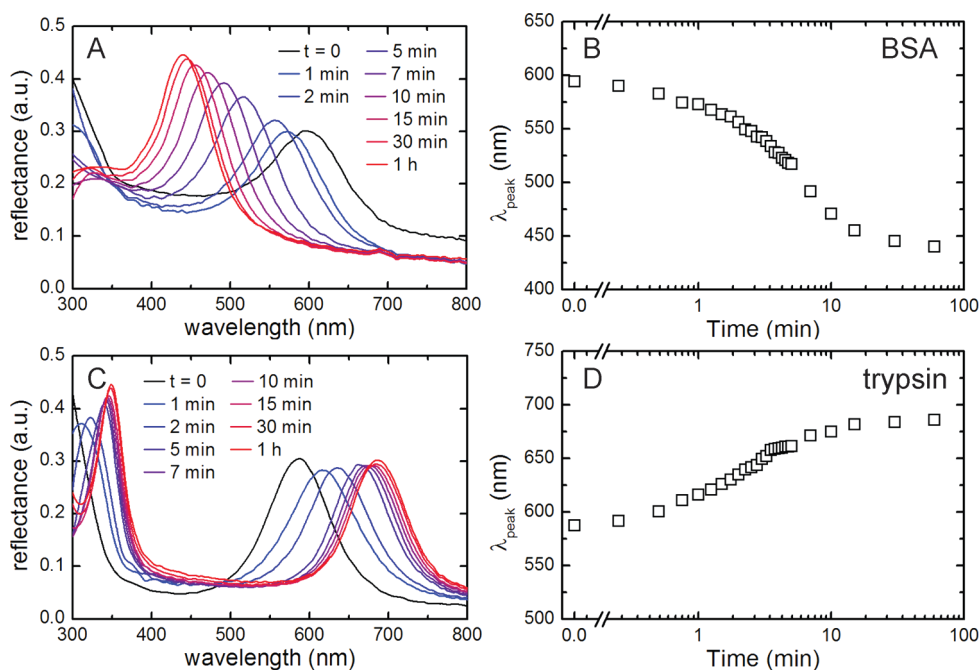


Figure 2. Real-time dynamic swelling spectra showing the blue shift in reflectivity of a PS-QP2VP photonic gel in 1 wt % BSA solution in 10 mM Tris buffer at pH 9 or the red shift in a 1% trypsin solution in 10 mM Tris buffer at pH 7 after soaking in the same buffer solution for 10 min. (A,C) Reflection spectra from $t = 0$ (equilibrium swelling in the buffer solution) to $t = 1$ h in the BSA or trypsin solution. (B,D) Peak reflectivity wavelengths as a function of the soaking time in the BSA or trypsin solution. The reflective peaks located at $\lambda/2$ are Bragg's peaks at (002) in the lamellar block copolymer photonic gels.

This clearly indicates that blue shifts are caused by the formation of coacervates, which causes the hydration of the QP2VP region to decrease, decreasing the hydrogel domain spacing and consequently the peak reflectivity wavelength. Increased pH results in an increasingly negative charge on BSA, yielding larger changes in wavelength (Figure S2). As the protein becomes more negatively charged, the protein–polymer coacervate will contain a lower protein content to maintain charge neutrality, and the QP2VP gel layer will be more dehydrated,³⁰ consistent with a larger blue shift. Although the dynamic changes in peak reflectivity wavelength are expected to be faster at higher pH because less protein is required to diffuse into the gel to reach a steady state, the time constants from fits to single-exponential functions do not show an obvious trend (Figure S2). The dynamic photonic response is governed by many coupled factors, such as interactions between different species, diffusion of proteins and counterions, protein size, gel thickness and concentration, as well as the formation of coacervates. In addition, the diffusion can take place from the film edge or through screw dislocation defects^{16,31} of the photonic gels, and the rate of transport will be modulated by coacervation as the gel swells/deswells. For the block copolymers used in this study, the bulk domain spacing is 56 nm,¹⁶ so the thickness of the QP2VP domain is significantly larger than a typical protein size of 5–8 nm even in the unswollen state. Therefore, protein diffusion is unlikely to be significantly restricted due to the size of the block copolymer domain. However, swelling of the

QP2VP domains increases the mesh size of the gel layer, resulting in more rapid transport of the protein. The interplay of these effects makes the dynamic response of the gels very complex.

In contrast, when a protein is below its isoelectric point, it has a net positive charge and may not be expected to interact strongly with the photonic gel. However, proteins are zwitterionic even when the total charge is net positive. In these molecules, induced charging, charge patches, and dipolar effects have been demonstrated to result in interactions between like charged proteins and polymers.^{30,32} The model protein, trypsin, has a negative zeta-potential at all three pH values but a positive calculated charge at pH 7 and a reported pI of 10. In contrast to gels exposed to BSA, gels exposed to trypsin red shift in the pH 7 solution and blue shift in the pH 8 and 9 solutions (Figure 2C,D and Figures S3 and S4). The results clearly indicate a strong interaction between trypsin and QP2VP; however, the effect of the interaction changes based upon the charge of the protein. When the protein is positively charged, it associates with the polymer chain; however, it is unable to collapse the polymer chain and, in fact, increases the total charge density within the gel. This increase in total charge density requires counterions to maintain charge neutrality, creating an increase in osmotic pressure in the gel and consequently an increase in swelling that is detected as a red shift in the peak reflectivity wavelength. However, as the charge is decreased with increasing pH, the protein becomes nearly neutral in charge and can

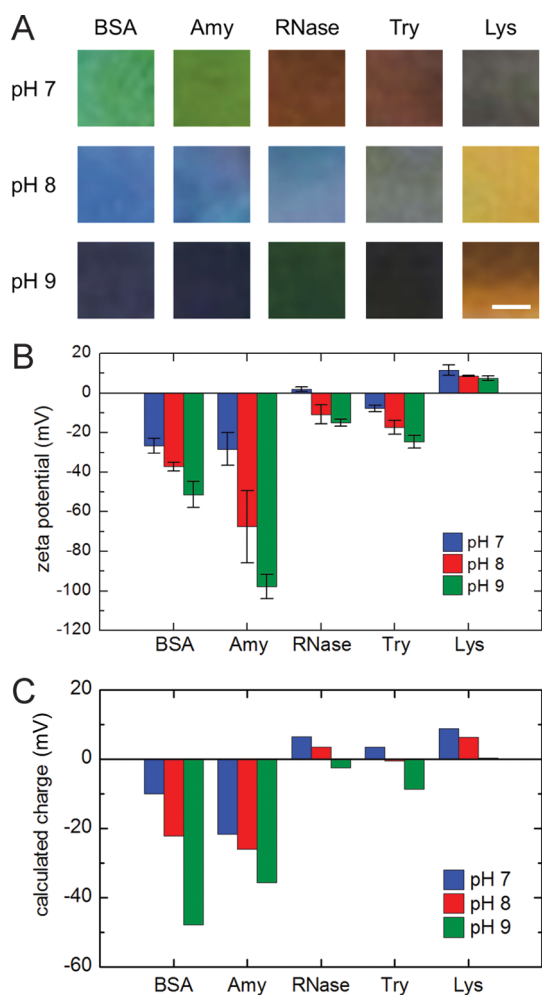


Figure 3. (A) Photos of PS-QP2VP photonic gels after soaking in 1% protein solutions in 10 mM Tris buffer overnight. Scale bar: 1 mm. (B) Experimentally measured zeta-potentials of the proteins in 10 mM Tris buffer. Error bars represent standard deviations from triplicated measurements. (C) Calculated formal charge based on amino acid sequence.

interact with the polymer by a more traditional counterion coacervation mechanism, resulting in a blue shift in the photonic gel. Although the photonic effect is observed to change direction around pH 8.0, loosely correlating with the calculated charge of trypsin, the charge distribution of a given protein is complex in nature and can be significantly altered by the surrounding environment, such as pH, various solvated ions, and ionic strength. Therefore, while the trend with changing charge is clear, the calculated charge is not believed to be quantitatively predictive in general.

Differences in pH-dependent responses between proteins can be used as a method to provide a fingerprint response for different biomolecules, as illustrated in Figure 3. A set of five widely available proteins with varying size, isoelectric point, and total charge was tested, although these parameters cannot be easily varied independently in natural proteins. While the magnitude of the photonic response correlates roughly with the pI of the proteins and the sign of the charge

strongly correlates with the direction of the photonic response, neither the total charge on the protein nor the protein size provides a strong correlation with the magnitude of the shift in peak wavelength. While coacervate phases typically form with charge-neutral mixtures of polyanions and polycations,^{33,34} the presence of dipolar interactions in proteins, induced charging effects, and the effects of nonionic interactions on equilibrium water content make theoretical prediction of the specific response to a given protein difficult. However, the response to a given protein can be measured and calibrated, enabling the change from a reference buffer spectrum to be used as a quantitative method of detection. Trypsin shows the largest change in peak reflectivity across the investigated pH range, while RNase has the second largest change. The theoretical charges of both of these proteins switch from positive to negative from pH 7 to 9, and zeta-potential measurements show that both transition from a small positive potential to a strong negative potential with increasing pH. This demonstration allows photonic response to be used as a tool to measure the “effective charges” of proteins. Proteins that undergo a larger change in absolute charge but are negatively charged at all pH values (BSA, amylase) show less pH dependence of the peak reflectivity, suggesting that the sensitivity of the photonic devices to changes in charge is greatest in the near neutral charge region.

Photonic responses induced by protein coacervation are significantly slower than solvent swelling of photonic gels due to the larger size of the protein molecules and due to interactions between protein and polymer that can further slow diffusion. While dry PS-QP2VP films swell quickly in aqueous buffers of monovalent salts to reach a steady-state reflectivity after only 10 s (Figure S5), the kinetics of swelling in response to protein is much slower and varies significantly depending upon the identity of the protein, as illustrated in Figure 2. Similar time scale contrasts are observed in other protein solutions (Figure S6). The origin of this slower response may result from two effects. First, diffusion of larger proteins into the block copolymer may be hindered by increasing the size of the molecule. Although protein size increases only roughly as the 1/3 power of the protein molar mass for a dense globular configuration, RNase, which is the smallest protein, does display the smallest time constant for film equilibration. Lysozyme, the second smallest protein, is also relatively fast. Amylase, the second largest protein, has the largest time constant. This trend, while clearly not capturing all the physics, is consistent with an important contribution due to a protein size effect. In addition, interactions between protein and the polymer gel may slow diffusion. In particular, coacervation of nanodomains near the surface of the photonic stack can lead to densification of these domains, resulting in hindered diffusion as

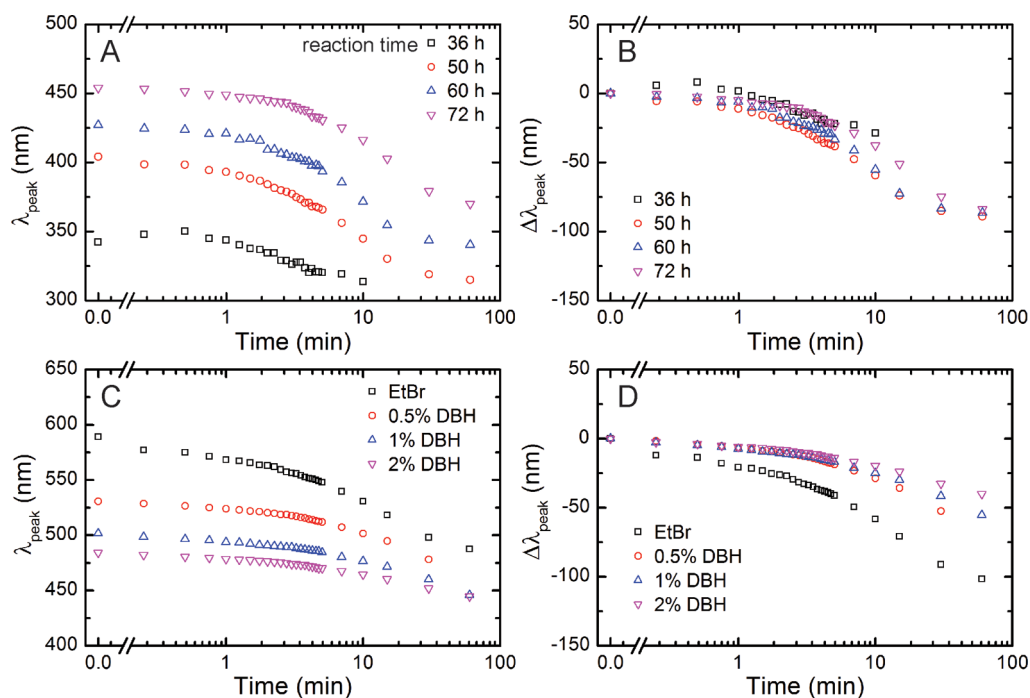


Figure 4. (A,B) Reflectivity peak wavelengths and peak shifts of PS-QP2VP photonic gels of various EtBr quaternization times swelling in 1 wt % BSA solution in 10 mM pH 9 Tris buffer. (C,D) Reflectivity peak wavelengths and peak shifts of PS-QP2VP photonic gels quaternized with EtBr/DBH mixtures swelling in the 1 wt % BSA solution in 10 mM pH 8 Tris buffer.

proteins must now pass through this dense layer in order to deswell subsequent layers. In this way, swelling is autoaccelerating as the addition of protein increases diffusivity through the gel, and deswelling is autoinhibitory as the addition of protein decreases diffusivity. This is consistent with shorter time constants in proteins where the gel expands rather than contracts. However, this effect is confounded by the fact that decreasing charge on the protein potentially enables a larger protein loading, increasing equilibration time. In both cases, thinner gels are anticipated to respond more quickly due to shorter diffusional distances; however, decreasing the number of photonic layers creates an engineering trade-off between reflectivity and response time.

Changes in the properties of the block copolymer photonic gel can also have a large impact on the swelling response when exposed to protein. The charge density of the QP2VP polycation affects the binding interaction and is one of the primary parameters for potential control of the responsive photonic effect. The charge density of the QP2VP polycation is determined by the conversion of the pyridines in the P2VP block, which can be controlled by altering the reaction time with the EtBr quaternization reagent. Figure 4 shows the dynamic swelling spectra of the photonic gels for PS-QP2VP films quaternized under different reaction times, where longer than 24 h quaternization is required in order to obtain a reflectivity peak in aqueous buffers at a wavelength >300 nm. Increasing the polymer charge density results in enhanced swelling in

aqueous buffer, but the shift in peak reflectivity wavelength is approximately identical when the films are exposed to protein.

Diffusion of proteins into the PS-QP2VP gel can be tuned by changing the mesh size within the gel layers *via* cross-linking of the QP2VP block. By using a difunctional bromide DBH as an additive to the quaternization reagent EtBr, the P2VP block can be quaternized and cross-linked in one step. Increasing the ratio of DBH to EtBr increases the cross-link density. Cross-linking results in a decrease in the swelling of the hydrogels in aqueous buffer; therefore, only a small amount of DBH can be added before the photonic gel's reflectivity peak drops below 300 nm and becomes undetectable. Regardless of cross-link density, all samples show blue shifts in reflectivity after being transferred to BSA solutions, indicating that cross-linking or the change in gel layer mesh size does not alter the sign of the interaction between the protein and the QP2VP gel block. However, increasing cross-linking density decreases the size of the shift in peak position. The dynamic changes in the reflectivity at different cross-linking conditions are fitted to single-exponential functions. For low concentrations of the cross-linker, it is found that the time constants increase with increasing cross-linking density, changing from 11.9 ± 0.8 s in the case of no cross-linker to 36.3 ± 6.9 s with 2% added cross-linker (Supporting Information). The results demonstrate an effective means for controlling the swelling/deswelling kinetics by changing the mesh size in the photonic gels. The response rate of

the photonic gels could be further accelerated by increasing the hydrophilicity of the P2VP layer to increase swelling and gel mesh size (for example, using methyl iodine in the quaternization reaction), driving protein transport with an external field, or increasing the temperature.

CONCLUSIONS

Coacervation is demonstrated as an effective method to modulate the peak reflectivity of block copolymer photonic gels, where complexation between a charged domain in the block copolymer and a charged protein provides a novel mechanism for responsive actuation of

the optical properties of the material. While proteins with a strong negative charge result in strong counterion interactions with the polycationic QP2VP blocks of block copolymers and a consequent decrease in swelling, proteins with a positive charge also show some effect. The dynamics of the process can be quantified, showing that the mesh size (cross-link density) of the polymer gel and the size of the protein play important roles in governing the dynamics of the process. This method therefore provides a simple optical readout to detect differences between proteins on the basis of parameters such as size and charge, providing a visual “fingerprint” for the protein properties.

EXPERIMENTAL SECTION

Materials. A PS-P2VP diblock copolymer with a number-average molecular weight of 102 kg mol^{-1} for the PS block, 97 kg mol^{-1} for the P2VP block, and polydispersity of 1.12 was purchased from Polymer Source, Inc. Propylene glycol monoether acetate (PGMEA, Alfa Aesar) and chloroform (Mallinckrodt) were used for the copolymer film preparation. Bromoethane and 1,6-dibromohexane were purchased from Aldrich. Five proteins (bovine serum albumin, α -amylase, ribonuclease A, trypsin, and lysozyme) were purchased from various suppliers as listed in Table 1. All chemicals and proteins were used as received unless otherwise noted.

PS-QP2VP Photonic Gels. PS-P2VP solutions (5 wt %) in PGMEA were used for film-casting onto glass microscope slides. The BCP solution was spread onto the slide with a glass Pasteur pipet and spin-cast at 500 rpm with a 5 s ramp for 90 s. The film was then annealed overnight in chloroform vapor at 50°C . The annealed samples were quaternized in heptane solutions containing 10 vol % EtBr or mixtures of bromoethane with DBH (Figure 1). The reactivity of the bromides is assumed to be constant in the different EtBr/DBH mixtures because of the low amounts of DBH (0.5 to 2 mol % of EtBr). The reactions took place at 50°C for 3 days unless otherwise noted. After the reactions ended, the samples were washed with ethanol to remove the reagents. This procedure has been previously established to yield a high degree of quaternization in PS-P2VP copolymer films.¹¹

Characterization of Real-Time Response of Photonic Gels in Various Protein Solutions. Protein solutions were freshly prepared in 10 mM Tris buffer at pH 7, 8, and 9 to reach a final concentration of 1 wt %. Tris buffer is selected to control pH because of its low ionic valency. The 10 mM concentration is low enough that the ionic strength of the buffer does not overshadow the ionic interactions between the protein and the QP2VP gel block.

Time-dependent reflection spectra were measured with an Ocean Optics HR4000CG-UV-NIR high-resolution spectrometer. The successive spectra (over the range of 300–800 nm) were collected at the beginning of the swelling process of the

PS-P2VP gels to capture the short time responses, and the single spectra were collected in the later stage with intervals longer than 3 min between the time points. For successive spectra, the high-speed acquisition mode was selected with 5 ms integration time and 10 scans to average, thus an interval of 50 ms between the successive spectra. The single spectra were saved with 5 ms integration time and 100 scans to average.

A quartz cuvette was filled with the buffer or protein solution, and the annealed and quaternized sample was inserted along the optical wall with the film side facing the solution. A blank glass slide immersed in the solution was used as the baseline. The dry sample was first soaked in the buffer solution for 10 min. The spectrum over the first minute was recorded as a reference for the solvent transport and film defect density,^{16,31} and a single spectrum was saved at the end of the 10 min equilibration period as the $t = 0$ point. The swollen sample was immediately transferred into a separate cuvette containing the protein solution. Successive spectra over the first 5 min were recorded, followed by single spectra taken at $t = 7, 10, 15, 30$ min, and the end of each hour. For each sample, the buffer solution and the protein solution had the same pH and buffer composition so that the data could be used to analyze the role of proteins on the photonic responses. All spectra were collected in transmission mode. The reflectance was calculated from the transmittance by $R = 1 - T$, assuming no absorption and no diffuse scattering.

Measurement of Protein Zeta-Potentials. Zeta-potential measurements were performed on Möbiu ζ with an Atlas pressurization system (Wyatt Technology). The protein solutions were freshly prepared at a concentration of 1 mg/mL in 10 mM Tris buffer and were centrifuged at 14 200g for 5 min. Since the protein sizes in this study were close to the Debye length in the buffer solution, the zeta-potential values were calculated using the built-in Henry's function instead of Smoluchowski's equation.

Conflict of Interest: The authors declare no competing financial interest.

Acknowledgment. The authors thank the U.S. Army Natick Soldier Research, Development and Engineering Center for funding support of this research.

Supporting Information Available: Time-dependent photonic gel responses to various proteins as a function of pH and fits to extract characteristic time constants for equilibration. This material is available free of charge via the Internet at <http://pubs.acs.org>.

TABLE 1. Proteins and Their Molar Weights and Isoelectric Points (pI)

protein	acronym	MW (kDa)	pI ^a	supplier
albumin from bovine serum	BSA	66	5.3	Sigma-Aldrich
α -amylase from <i>Aspergillus oryzae</i>	Amy	51	4.48 ^a	Sigma-Aldrich
ribonuclease A (bovine pancreas)	RNase	13.7	9.63	Amresco
trypsin from porcine pancreas	Try	23.8	10	Sigma-Aldrich
lysozyme from chicken egg white	Lys	14.3	11.35	Sigma-Aldrich

^a The pI value of α -amylase is estimated using the online software from http://web.expasy.org/compute_pi/. The amino acid sequence of α -amylase is from PDB file 6TAA. All other pI values are provided by the protein suppliers.

REFERENCES AND NOTES

- Baker, N. A.; Sept, D.; Joseph, S.; Holst, M. J.; McCammon, J. A. Electrostatics of Nanosystems: Application to Microtubules and the Ribosome. *Proc. Natl. Acad. Sci. U.S.A.* **2001**, *98*, 10037–10041.
- Vukusic, P.; Sambles, J. R. Photonic Structures in Biology. *Nature* **2003**, *424*, 852–855.

3. Kinoshita, S.; Yoshioka, S. Structural Colors in Nature: The Role of Regularity and Irregularity in the Structure. *ChemPhysChem* **2005**, *6*, 1442–1459.
4. Zi, J.; Yu, X. D.; Li, Y. Z.; Hu, X. H.; Xu, C.; Wang, X. J.; Liu, X. H.; Fu, R. T. Coloration Strategies in Peacock Feathers. *Proc. Natl. Acad. Sci. U.S.A.* **2003**, *100*, 12576–12578.
5. Vigneron, J. P.; Colomer, J. F.; Rassart, M.; Ingram, A. L.; Lousse, V. Structural Origin of the Colored Reflections from the Black-Billed Magpie Feathers. *Phys. Rev. E* **2006**, *73*.
6. Huang, J. Y.; Wang, X. D.; Wang, Z. L. Controlled Replication of Butterfly Wings for Achieving Tunable Photonic Properties. *Nano Lett.* **2006**, *6*, 2325–2331.
7. Kolle, M.; Salgard-Cunha, P. M.; Scherer, M. R. J.; Huang, F. M.; Vukusic, P.; Mahajan, S.; Baumberg, J. J.; Steiner, U. Mimicking the Colourful Wing Scale Structure of the *Papilio blumei* Butterfly. *Nat. Nanotechnol.* **2010**, *5*, 511–515.
8. Galusha, J. W.; Richey, L. R.; Gardner, J. S.; Cha, J. N.; Bartl, M. H. Discovery of a Diamond-Based Photonic Crystal Structure in Beetle Scales. *Phys. Rev. E* **2008**, *77*.
9. Kramer, R. M.; Crookes-Goodson, W. J.; Naik, R. R. The Self-Organizing Properties of Squid Reflectin Protein. *Nat. Mater.* **2007**, *6*, 533–538.
10. Joannopoulos, J. D. *Photonic Crystals: Molding the Flow of Light*, 2nd ed.; Princeton University Press: Princeton, NJ, 2008.
11. Kang, Y.; Walsh, J. J.; Gorishnyy, T.; Thomas, E. L. Broad-Wavelength-Range Chemically Tunable Block-Copolymer Photonic Gels. *Nat. Mater.* **2007**, *6*, 957–960.
12. Walsh, J. J.; Kang, Y.; Mickiewicz, R. A.; Thomas, E. L. Bioinspired Electrochemically Tunable Block Copolymer Full Color Pixels. *Adv. Mater.* **2009**, *21*, 3078–3081.
13. Chan, E. P.; Walsh, J. J.; Thomas, E. L.; Stafford, C. M. Block Copolymer Photonic Gel for Mechanochromic Sensing. *Adv. Mater.* **2011**, *23*, 4702–4706.
14. Walsh, J. J.; Fan, Y.; Centrone, A.; Thomas, E. L. Controlling Thermochromism in a Photonic Block Copolymer Gel. *Macromol. Rapid Commun.* **2012**, *33*, 1504–1509.
15. Lim, H. S.; Lee, J. H.; Walsh, J. J.; Thomas, E. L. Dynamic Swelling of Tunable Full-Color Block Copolymer Photonic Gels via Counterion Exchange. *ACS Nano* **2012**, *6*, 8933–8939.
16. Fan, Y.; Walsh, J. J.; Tang, S. C.; Olsen, B. D.; Thomas, E. L. Defects, Solvent Quality, and Photonic Response in Lamellar Block Copolymer Gels. *Macromolecules* **2014**, *47*, 1130–1136.
17. Xia, Y.; Olsen, B. D.; Kornfield, J. A.; Grubbs, R. H. Efficient Synthesis of Narrowly Dispersed Brush Copolymers and Study of Their Assemblies: The Importance of Side-Chain Arrangement. *J. Am. Chem. Soc.* **2009**, *131*, 18525–18532.
18. Sveinbjornsson, B. R.; Weitekamp, R. A.; Miyake, G. M.; Xia, Y.; Atwater, H. A.; Grubbs, R. H. Rapid Self-Assembly of Brush Block Copolymers to Photonic Crystals. *Proc. Natl. Acad. Sci. U.S.A.* **2012**, *109*, 14332–14336.
19. Yoon, J.; Lee, W.; Thomas, E. L. Thermochromic Block Copolymer Photonic Gel. *Macromolecules* **2008**, *41*, 4582–4584.
20. Osuji, C.; Chao, C. Y.; Bitá, I.; Ober, C. K.; Thomas, E. L. Temperature-Dependent Photonic Bandgap in a Self-Assembled Hydrogen-Bonded Liquid-Crystalline Diblock Copolymer. *Adv. Funct. Mater.* **2002**, *12*, 753–758.
21. Kim, E.; Kang, C.; Baek, H.; Hwang, K.; Kwak, D.; Lee, E.; Kang, Y.; Thomas, E. L. Control of Optical Hysteresis in Block Copolymer Photonic Gels: A Step towards Wet Photonic Memory Films. *Adv. Funct. Mater.* **2010**, *20*, 1728–1732.
22. Veis, A.; Aranyi, C. Phase Separation in Polyelectrolyte Systems 0.1. Complex Coacervates of Gelatin. *J. Phys. Chem.* **1960**, *64*, 1203–1210.
23. Weinbreck, F.; Tromp, R. H.; de Kruijff, C. G. Composition and Structure of Whey Protein/Gum Arabic Coacervates. *Biomacromolecules* **2004**, *5*, 1437–1445.
24. Chollakup, R.; Smitthipong, W.; Eisenbach, C. D.; Tirrell, M. Phase Behavior and Coacervation of Aqueous Poly(acrylic acid)-Poly(allylamine) Solutions. *Macromolecules* **2010**, *43*, 2518–2528.
25. Overbeek, J. T. G.; Voorn, M. J. Phase Separation in Polyelectrolyte Solutions. Theory of Complex Coacervation. *J. Cell. Physiol.* **1957**, *49*, 7–26.
26. Veis, A. A Review of the Early Development of the Thermodynamics of the Complex Coacervation Phase Separation. *Adv. Colloid Interface Sci.* **2011**, *167*, 2–11.
27. Krogstad, D. V.; Lynd, N. A.; Choi, S. H.; Spruell, J. M.; Hawker, C. J.; Kramer, E. J.; Tirrell, M. V. Effects of Polymer and Salt Concentration on the Structure and Properties of Triblock Copolymer Coacervate Hydrogels. *Macromolecules* **2013**, *46*, 1512–1518.
28. Voets, I. K.; de Keizer, A.; Stuart, M. A. C. Complex Coacervate Core Micelles. *Adv. Colloid Interface Sci.* **2009**, *147–148*, 300–318.
29. Kim, B.; Lam, C. N.; Olsen, B. D. Nanopatterned Protein Films Directed by Ionic Complexation with Water-Soluble Diblock Copolymers. *Macromolecules* **2012**, *45*, 4572–4580.
30. Cooper, C. L.; Dubin, P. L.; Kayitmazer, A. B.; Turksen, S. Polyelectrolyte-Protein Complexes. *Curr. Opin. Colloid Interface Sci.* **2005**, *10*, 52–78.
31. Lee, J.-H.; Koh, C. Y.; Singer, J. P.; Jeon, S.-J.; Maldovan, M.; Stein, O.; Thomas, E. L. 25th Anniversary Article: Ordered Polymer Structures for the Engineering of Photons and Phonons. *Adv. Mater.* **2014**, *26*, 532–569.
32. Park, J. M.; Muhoberac, B. B.; Dubin, P. L.; Xia, J. L. Effects of Protein Charge Heterogeneity in Protein-Polyelectrolyte Complexation. *Macromolecules* **1992**, *25*, 290–295.
33. Hiemenz, P. C.; Rajagopalan, R. *Principles of Colloid and Surface Chemistry*, 3rd ed.; Marcel Dekker: New York, 1997.
34. Russel, W. B.; Saville, D. A.; Schowalter, W. R. *Colloidal Dispersions*; Cambridge University Press: Cambridge, 1989.